Effect of symmetry breaking on the optical absorption of semiconductor nanoparticles

Adam Gali*
Research Institute for Solid State Physics and Optics, Hungarian Academy of Sciences, P.O. Box 49, H-1525 Budapest, Hungary and Department of Atomic Physics, Budapest University of Technology and Economics, Budafoki út 8, H-1111 Budapest, Hungary

Efthimios Kaxiras
Department of Physics and School of Engineering and Applied Sciences, Harvard University, Cambridge, Massachusetts 02138, USA

Gergely T. Zimanyi
Physics Department, University of California, Davis, California 95616, USA

Sheng Meng†
Beijing National Laboratory for Condensed Matter Physics and Institute of Physics, Chinese Academy of Sciences, Beijing 100190, China
(Received 8 February 2011; published 29 July 2011)

The shape of semiconductor nanoparticles (NPs) can have an important influence on their optical absorption spectra with enhanced absorption resulting from breaking their symmetries. To illustrate this effect, we present broad energy optical excitation spectra of ∼2 nm Si and PbSe nanoparticles, obtained from extensive time-dependent density functional theory calculations. We considered both highly symmetric spherical shapes and low-symmetry rodlike and disklike shapes. The low-symmetry shapes exhibit an increase in absorption at low and relatively high energies compared to the absorption of spherical NPs of similar volume, independent of their chemical compositions and surface structures. Our results elucidate the mechanism of enhanced multiexciton generation in semiconductor NPs, which is important in the quest to improve their photovoltaic applications.

DOI: 10.1103/PhysRevB.84.035325 PACS number(s): 78.67.Bf, 71.15.Qe, 73.22.−f, 78.40.Fy

I. INTRODUCTION

In the quest for more efficient photovoltaic (PV) devices, the development of new materials and processes can play a crucial role. In particular, systems that can take advantage of the physics of nanoscale structures may introduce new possibilities and lead to breakthroughs in solar energy harvesting and conversion.[1] An exciting possibility is the generation of multiple electron-hole pairs by each photon absorbed, a process referred to as "multiexciton generation" (MEG), which has been observed in semiconductor nanoparticles (NPs);[2–10] this would increase their current and useful power output. MEG could actually be enhanced in NPs relative to the bulk material, further improving device efficiency. The physics behind this enhancement is the suppression of exciton decay by phonon emission in NPs (the "phonon bottleneck") due to the reduced number of available vibrational states and the more facile creation of additional excitons due to stronger Coulomb interaction in NPs from less efficient screening. Recent studies on II-VI and III-V NPs found that MEG efficiencies are smaller than originally suggested[11–17] and depend on surface chemistry, NP concentration, and measurement conditions that can lead to charging.[18–23] While the degree of enhancement is debated by these authors, all of them agree that MEG does occur in PbSe.[14,17,23]

Energy conservation implies that MEG can only be induced by an incident photon with energy $h\nu \geqslant mE_g$, where E_g is the optical gap and m an integer greater than 2. Biexciton creation ($m = 2$) is considered the optimal scenario for PV applications because the exciton lifetime decreases with increasing m,[4] and the extraction of multiple excitons is challenging.[24] Moreover, typical semiconductor band gaps are in the range of 1 eV, and the solar spectrum intensity peaks in the range of 1.4–3.0 eV, making MEG with $m = 2$ or 3 the only practically relevant cases. For higher efficiency in solar energy conversion, the threshold energy for biexciton creation, E_{thr}, should be as close to the theoretical limit of $2E_g$ as possible, but it is larger in experiments.[4] The ratio E_{thr}/E_g depends on the material, the size, and the surface of the NP. Intriguingly, with decreasing NP size, this ratio can be reduced: for instance, it is about 4.2 for the bulk and 2.7 for the NPs of PbSe.[25] Effects that increase the value of this ratio in bulk processes are the curvature of the band structure, the splitting of energy levels close to E_g, indirect transitions, and the selection rules for optical excitation that are imposed by translational symmetry; the relaxation of selection rules in NPs can help bring this ratio closer to the desired limit.[25] On the other hand, the finite size of NPs leads to quantum confinement and consequently a larger E_g compared to the bulk. This fact can have an effect opposite to the trends mentioned thus far: for instance, the number of excitons created by a photon at a specific excitation energy is larger in bulk than in NPs of PbSe,[26,27] due to the quantum-confinement-induced lower density of states in the NPs at the given excitation energy. A thorough understanding of the physics behind these effects is the key to improving MEG in NPs and to exploiting materials that otherwise may appear to be unsuitable for PV applications given their bulk properties.

In this work, we show through extensive first-principles calculations of optical properties that taking advantage of the symmetry of NPs can prove very effective in addressing some of the issues raised above. Semiconductors typically exhibit O_h symmetry in the bulk, which is reduced to T_d in NPs of spherical shape. The T_d group, one of the highest symmetries among the three-dimensional (3D) crystallographic point groups, leads to a large number of selection rules with many dipole transitions forbidden to first order. Thus, in highly

symmetric NPs, crystal momentum selection rules may not be relaxed sufficiently, particularly for larger sizes.[28] Reducing the symmetry of the NPs can lift more selection rules for dipole transitions, opening new channels for photon absorption. This can be achieved by distorting the spherical shape toward rodlike (elongated in one dimension) or disklike (elongated in two dimensions) shapes. NPs of such shapes have already been fabricated,[29–34] but only their low-energy excitation spectra have been studied and analyzed in detail.[35–39]

To illustrate our point, we selected two materials in which the atomic coordination, the nature of bonds, and the crystal lattice are all different, namely, Si (with fourfold tetrahedral covalent bonds in the diamond lattice) and PbSe (with sixfold cubic ionic bonds in the rock salt lattice). We considered NPs of these materials of various shapes, including spherical, rodlike, and disklike, and of approximately constant volume (corresponding to an ∼2 nm diameter for the spherical shape) and show thorough time-dependent density functional theory (TD-DFT) calculations of the optical absorption spectra that the lower-symmetry shapes (rods and disks) have higher absorption in the energy range E_g to $3E_g$, independent of their chemical compositions and surface structures.

II. METHODOLOGY

We used the local-basis approach as implemented in the SIESTA code[40] and norm-conserving pseudopotentials[41] with periodic cells in which the closest distance between surface atoms of the periodic images was larger than 1 nm; all structures were fully relaxed. As a check, we also performed plane-wave calculations with the VASP code[42] and found excellent agreement between the results of the two different approaches. Absorption spectra were obtained from TD-DFT,[43] with the generalized gradient Perdew-Burke-Ernzerhof functional[44] in the exchange-correlation kernel. For relatively small NPs, TD-DFT provides a qualitatively correct description of excitation processes (unlike for the case of bulk solids) and is used here to discuss trends in the excitation spectra of Si and PbSe NPs as a function of their shapes. The implementation of the TD-DFT method within the SIESTA code is described in Refs. 45 and 46 in detail, where this method was applied for both molecules and small hydrogenated Si and Ge nanoclusters. In recent years, other TD-DFT codes have been applied to hydrogenated Si and Ge nanoclusters (for example, the authors of Refs. 47–49 discuss results very similar to those obtained with our implementation).[46] In this study we apply the TD-DFT method for the well-known hydrogenated Si and the less-known PbSe nanoclusters. Spin-orbit interactions play an important role in PbSe due to the heavy Pb nuclei[50] and can significantly reduce the calculated fundamental gap of ∼2 nm PbSe NPs,[51] but do not affect the geometry. Computationally, it is prohibitive to calculate the TD-DFT excitation spectrum including spin-orbit coupling for relatively large nanoclusters while a simple DFT optical spectrum yields qualitatively wrong results. Thus, we calculated the excitation spectra of PbSe NPs without spin-orbit coupling and discuss below the error from this approximation.

We note here that the TD-DFT method provides absorption spectra with semi-quantitative accuracy for semiconductor nanoclusters but does not yield the MEG efficiencies directly. It has been shown that impact ionization may explain the MEG, particularly in PbSe nanoclusters.[52–55] The calculation of impact ionization within the perturbation approach needs the evaluation of about 2 000 000 Coulomb integrals between Kohn-Sham states in a relatively small $Si_{66}H_{64}$ nanocrystal for the appropriate energy range of biexciton generation. In addition, the dielectric function of this cluster must also be determined accurately, a calculation which is computationally demanding. Technically, it is currently impossible to calculate the MEG fully *ab initio* for the sizes where the shape effects can be calculated by the TD-DFT shown in this paper. Thus, we argue that if the intensity of absorption is larger, the MEG is larger as the available biexcitonic states grow quadratically with increasing number of available joint density of states while the single-exciton states only grow linearly. Recent tight-binding calculations support this view.[56] We notice that our recent full *ab initio* calculations of MEG also support our argument in small hydrogenated silicon nanoclusters.[57]

III. RESULTS

We first discuss the Si NPs [Fig. 1]. We built the spherical NP structure ($Si_{220}H_{144}$, labeled A1) under the constraints that it should exhibit T_d symmetry and that every surface Si atom should be covalently bonded to at least two other Si atoms with the dangling bonds passivated by H atoms. Hydrogenated Si NPs have been recently fabricated, and it has been argued that these NPs are ideal for studying excitons experimentally.[58] MEG in Si NPs was measured in a hexane solvent where the surface was presumably partially terminated by carbon chains. The high-energy excitation spectrum of Si NPs with carbon chains at the surface differs from the hydrogenated one,[59] but including carbon-chain termination would increase the computational cost beyond what is currently feasible. Moreover, the *difference* in the calculated spectra of different shapes but with the same surface termination, which is

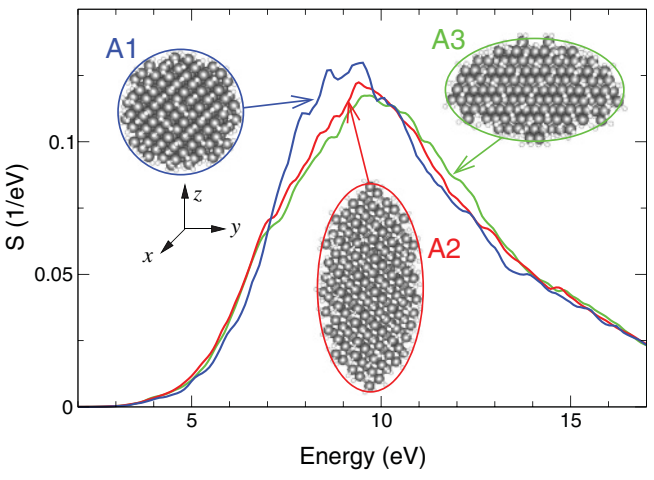

FIG. 1. (Color online) Optical absorption spectra of the Si NPs with spherical (A1), rodlike (A2), and disklike (A3) shapes. The three atomic structures are shown as insets (Si atoms, gray spheres; H atoms, white spheres). The colored ellipses (circle for A1) show the approximate cross section on a plane containing one of the two equivalent directions (x, y) and the inequivalent direction (z) of the lower-symmetry A2 and A3 structures.

the key quantity of interest here, should be qualitatively similar for different surface terminations of Si NPs. We built the lower-symmetry rodlike ($Si_{219}H_{156}$, A2) structures and disklike ($Si_{195}H_{148}$, A3) structures with the constraint that their volumes should be almost equal to the volume of the spherical structures and have the same surface constraints as in the spherical case. In the A2 structure, the diameter along the z direction is 2.8 nm and 1.7 nm along the x and y directions; the corresponding values for A3 are 1.0 and 2.4 nm.

The calculated excitation spectra of Si NPs with different shapes are shown in Fig. 1. The absorption intensity is higher in rod- and disklike shapes than in the spherically shaped Si NPs up to a characteristic energy of excitation above which the trend is the opposite. For the NPs considered here, this characteristic energy is $\sim 3E_g$, demonstrating that the overall absorption can be increased in the E_g to $3E_g$ energy range relevant for PV applications. The rod- and disklike shapes show very similar characteristics. The optical gap is the same within 0.08 eV for all the shapes (A1, 2.12 eV; A2, 2.06 eV; and A3, 2.14 eV) as expected, since the deviation from the spherical shape is relatively small. The increase in the intensity of absorption in low-symmetry Si NPs can be partially explained by the relaxation of selection rules. An intuitive explanation is based on invoking quantum confinement effects: The NPs can be modeled by quantum boxes with infinitely large potential barriers; a simple analytical argument shows that the most symmetric quantum box (cube) has the lowest absorption compared to that of a general rectangular quantum box. In the case of low-symmetry NPs, the low-lying energy states are less confined while the high-energy empty states are more confined along the short axes of the NPs. This simple argument is actually borne out by our DFT calculations for the confinement of states in Si and PbSe NPs. By integrating the absorption spectrum in the E_g to $3E_g$ energy range, we obtain an enhancement of about 25% for the rodlike NPs (20% for the disklike ones) relative to the spherical NPs. These results indicate a larger number of exciton states in the rodlike and disklike Si NPs. In addition, E_{thr} might be reduced due to the lower symmetry of the system.

It is instructive to study the polarization dependence of the spectra for axially symmetric shapes in comparison to the spectrum of the spherical NPs (see Fig. 2). The absorption is different along the z direction and along the x and y directions of the rodlike (red curve, right graph) and disklike (green curve, left graph) Si NPs, as expected from their symmetry. In the case of the rodlike Si NPs, the absorption is larger for light polarized along the z direction than along the x and y directions in the relevant energy region. A previous tight-binding study found this effect in Si nanoclusters.[60] We explain this behavior by simple quantum confinement arguments as mentioned earlier: along the elongated z axis, the quantum confinement is considerably smaller than along the other axes. Thus, the electron states close to the gap are delocalized along the entire nanorod, which can absorb z-polarized light of greater intensity. The states confined strictly across the nanorod ($x-y$ plane) are split by a much larger energy than the fundamental gap, and consequently the absorption polarized along the x and y directions is more intense at higher energies. This simple explanation is in line with the relative absorption intensities of a spherical NP versus

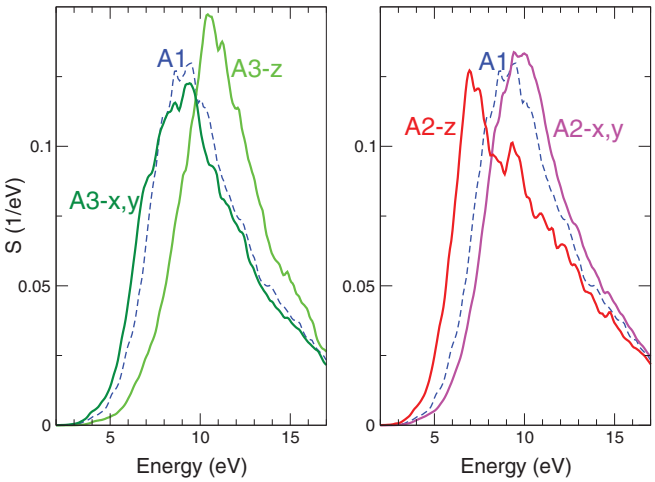

FIG. 2. (Color online) Polarization-resolved absorption spectra of the low-symmetry Si nanoparticles A2 and A3. Axial directions are defined in Fig. 1. For comparison, the spectrum of A1 is also shown as dashed lines.

a rodlike NP. In the disklike NPs, the quantum confinement is stronger along the z direction than in the other directions, and the corresponding polarization dependence follows the pattern explained above: the absorption intensity is stronger at lower energies for light polarized along the x and y directions while the absorption intensity along the z direction dominates at higher energies. These results suggest that proper orientation of the nonspherical NPs can lead to optimized absorption in PV devices.

We turn next to PbSe NPs, all with the same composition, $Pb_{68}Se_{68}$ (Fig. 3). We used the bond center as the origin to build the various structures, which automatically results in stoichiometric NPs with the full T_d symmetry retained for the spherical (B1) structure. The creation of a stoichiometric structure ensures that there are no artifacts in the electronic structure such as deep gap states.[61] We followed a similar procedure to that employed for the Si NPs to construct stoichiometric rodlike (B2) and disklike (B3) PbSe NPs. In the B2 structure, the diameter along the z direction is 2.2 nm while it is 1.6 nm along the x and y directions; the corresponding values for B3 are 0.9 and 2.2 nm. Colloidal PbSe NPs exist in organic solvents (such as tetrachlorethylene), but there is no evidence from experiments or theory that covalent bonds are formed between the molecules of the solvent and the ionic PbSe particles. Thus, we did not use any surface passivation in PbSe NPs but allowed the surface atoms to relax to find the minimum energy structure.

In bulk form, PbSe is very different from Si: it has a much lower band gap, the rocksalt crystal structure, ionic bonds between the constituent atoms, and a nonreactive surface. Despite all of these differences, the basic features of the calculated absorption spectra of PbSe NPs [Fig. 3(a)] are similar to those of the Si NPs. The absorption intensity is higher in rod- and disklike shapes than in spherically shaped PbSe NPs up to a characteristic energy of excitation though the enhancement in absorption is more pronounced for rodlike than for disklike PbSe NPs. In the PbSe NPs we considered, this characteristic energy is well above $3E_g$ (it is close to $5E_g$),

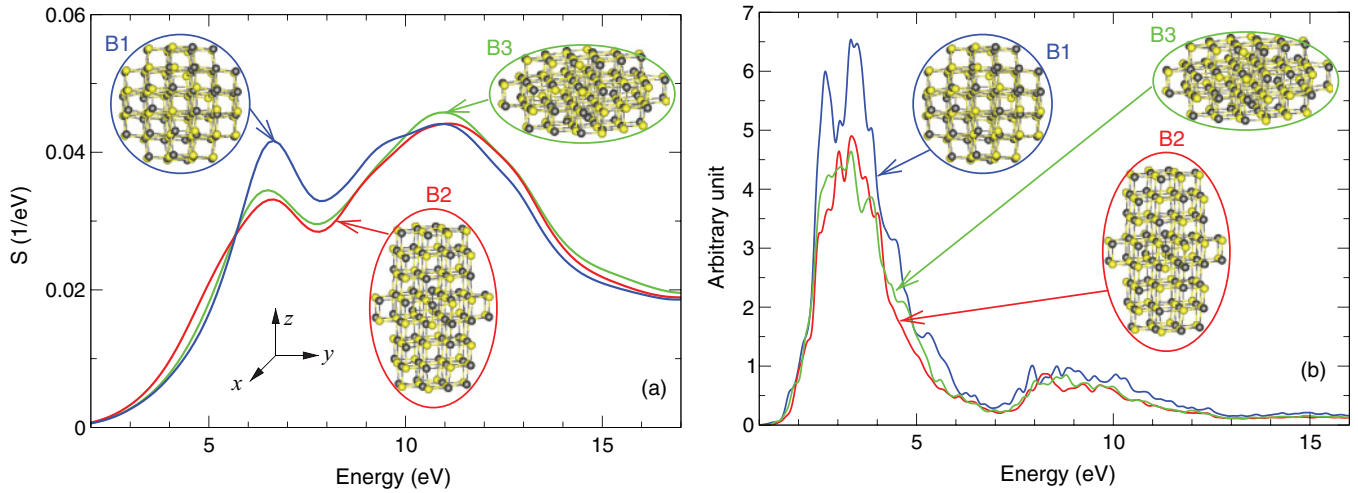

FIG. 3. (Color online) Optical absorption spectra of the PbSe NPs with spherical (B1), rodlike (B2), and disklike (B3) shapes. The three atomic structures are shown as insets [Pb atoms, (gray) dark spheres; Se atoms, (yellow) light spheres]. Other notation is similar to that in Fig. 1. (a) TD-DFT spectra and (b) DFT spectra.

which shows that the overall absorption can be increased in the E_g to $3E_g$ energy range relevant to PV applications. The optical gap is the same within 0.2 eV for all the shapes (B1, 1.25 eV; B2, 1.13 eV; and B3, 1.33 eV). There is a dip in the calculated excitation spectra of PbSe NPs at very high energy, 7.5 eV, characteristic for all shapes. We attribute this dip to the energy gap between the valence Se p states and the Pb s states. While the energy gap between Pb s and Se p states may decrease by using more accurate methods, Pb s orbitals do not seem to play a role in absorption in the visible part of the solar cell spectrum. By integrating the absorption spectrum in the E_g to $3E_g$ energy range for our PbSe NPs, we obtain an enhancement of about 31% for the rodlike (7% for the disklike) PbSe NPs relative to the spherical ones. The increase in the absorption at low energy may be again explained by quantum confinement arguments similar to the case of Si NPs though this effect is not as pronounced for PbSe NPs due to the hybridization of the bulklike states with the surface states (see Fig. 4). The polarization dependence of the absorption spectra of PbSe NPs is very similar to that of Si NPs. The density of states of the PbSe NPs increases in the energy range about 1–2 eV below the highest occupied state in the rodlike and disklike PbSe NPs relative to that of the spherical PbSe NPs. These states are associated with Se p orbitals and are localized on atoms along the elongated axis of the PbSe NPs; they contribute to the increase of absorption in the relevant energy range important for PV applications.

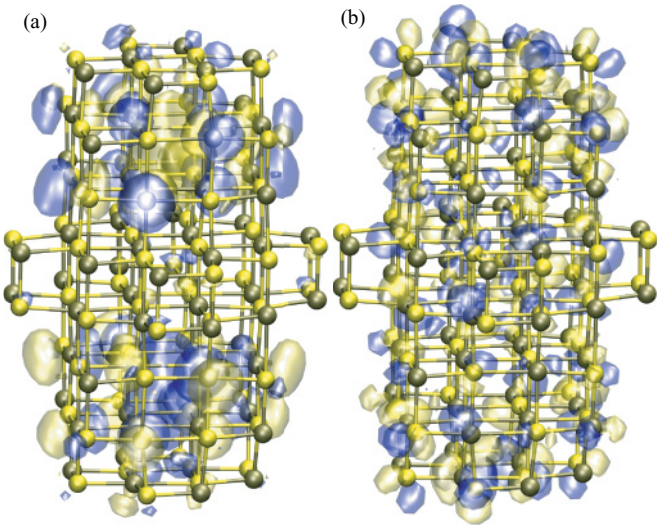

FIG. 4. (Color online) Selected wave functions of empty levels in a rodlike PbSe NP (a) at low-end energy (E_g) and (b) at high-end energy ($4E_g$) with respect to the highest occupied molecular orbital. Light (yellow) and dark (blue) lobes represent the isosurface of the positive and negative values of the selected wave functions, respectively. Pb atoms, (gray) dark spheres; Se atoms, (yellow) light spheres.

Finally, we comment on the error introduced by the neglect of spin-orbit coupling. Again, we emphasize that DFT provides qualitatively wrong excitation spectra giving incorrect shapes of spectra as demonstrated in Fig. 3. Thus, we chose to use TD-DFT but to neglect spin-orbit coupling in contrast to a previous work.[51] This coupling is effective on the Pb p orbitals located in the "conduction band" (the unoccupied NP states) and would shift the calculated E_g to lower values, affecting the optical spectrum. We expect that the shape dependence of the spectrum will not change qualitatively because the enhancement of absorption in the rodlike and disklike shapes is mostly due to quantum confinement effects, which do not depend on the spin state but rather on the spatial localization of the wave functions. Moreover, as we discussed above, this quantum confinement will mostly change the density of states in the "valence band" associated with Se p orbitals in which spin-orbit coupling is negligible.

IV. SUMMARY

In summary, we have investigated high-energy excitations in Si and PbSe NPs using TD-DFT methods. We demonstrated that rodlike and disklike nanoparticles show enhancement in their absorption at energies of excitation at which excitons and

biexcitons can be created, relative to the absorption of spherical nanoparticles with the same volume. We also provided insight into the polarization dependence of the absorption of nonspherical nanoparticles. Shape manipulation of nanoparticles opens a route to maximize the overall absorption at a given volume and could possibly reduce the threshold energy for exciton generation. Our findings should assist in the design of nanoscale structures that exhibit enhanced MEG, possibly proving useful for more efficient solar energy conversion.

ACKNOWLEDGMENTS

A.G. acknowledges support from the Hungarian OTKA Grant No. K-67886, the János Bolyai program from the Hungarian Academy of Sciences, and the NHDP program Grant No. TÁMOP-4.2.1/B-09/1/KMR-2010-0002. S.M. acknowledges partial financial support from the Hundred Talent Program of CAS and NSFC (Grant No. 11074287). G.T.Z. acknowledges the support of NSF-SOLAR Grant No. 1035468.

*agali@eik.bme.hu
†smeng@iphy.ac.cn

[1] A. J. Nozik, Physica E **14**, 115 (2002).
[2] R. D. Schaller and V. I. Klimov, Phys. Rev. Lett. **92**, 186601 (2004).
[3] R. J. Ellingson, M. C. Beard, J. C. Johnson, P. Yu, O. I. Micic, A. J. Nozik, A. Shabaev, and A. L. Efros, Nano Lett. **5**, 865 (2005).
[4] R. D. Schaller, V. M. Agranovitch, and V. I. Klimov, Nature Phys. **1**, 189 (2005).
[5] R. D. Schaller, M. A. Petruska, and V. I. Klimov, Appl. Phys. Lett. **87**, 253102 (2005).
[6] S. J. Kim, W. J. Kim, Y. Sahoo, A. N. Cartwright, and P. N. Prasad, Appl. Phys. Lett. **92**, 031107 (2008).
[7] R. D. Schaller, M. Sykora, S. Jeong, and V. I. Klimov, J. Phys. Chem. B **110**, 25332 (2006), pMID: 17165979.
[8] J. J. H. Pijpers, E. Hendry, M. T. W. Milder, R. Fanciulli, J. Savolainen, J. L. Herek, D. Vanmaekelbergh, S. Ruhman, D. Mocatta, D. Oron, A. Aharoni, U. Banin, and M. Bonn, J. Phys. Chem. C **111**, 4146 (2007).
[9] R. D. Schaller, J. M. Pietryga, and V. I. Klimov, Nano Lett. **7**, 3469 (2007).
[10] M. C. Beard, K. P. Knutsen, P. Yu, J. M. Luther, Q. Song, W. K. Metzger, R. J. Ellingson, and A. J. Nozik, Nano Lett. **7**, 2506 (2007).
[11] G. Nair and M. G. Bawendi, Phys. Rev. B **76**, 081304 (2007).
[12] J. J. H. Pijpers, E. Hendry, M. T. W. Milder, R. Fanciulli, J. Savolainen, J. L. Herek, D. Vanmaekelbergh, S. Ruhman, D. Mocatta, D. Oron, A. Aharoni, U. Banin, and M. Bonn, J. Phys. Chem. C **112**, 4783 (2008).
[13] M. Ben-Lulu, D. Mocatta, M. Bonn, U. Banin, and S. Ruhman, Nano Lett. **8**, 1207 (2008).
[14] M. T. Trinh, A. J. Houtepen, J. M. Schins, T. Hanrath, J. Piris, W. Knulst, A. P. L. M. Goossens, and L. D. A. Siebbeles, Nano Lett. **8**, 1713 (2008).
[15] G. Nair, S. M. Geyer, L.-Y. Chang, and M. G. Bawendi, Phys. Rev. B **78**, 125325 (2008).
[16] M. Ji, S. Park, S. T. Connor, T. Mokari, Y. Cui, and K. J. Gaffney, Nano Lett. **9**, 1217 (2009).
[17] J. J. H. Pijpers, R. Ulbricht, K. J. Tielrooij, A. Osherov, Y. Golan, C. Delerue, G. Allan, and M. Bonn, Nature Phys. **5**, 811 (2005).
[18] J. M. Luther, M. C. Beard, Q. Song, M. Law, R. J. Ellingson, and A. J. Nozik, Nano Lett. **7**, 1779 (2007).
[19] J. A. McGuire, J. Joo, J. M. Pietryga, R. D. Schaller, and V. I. Klimov, Acc. Chem. Res. **41**, 1810 (2008).
[20] G. I. Koleilat, L. Levina, H. Shukla, S. H. Myrskog, S. Hinds, A. G. Pattantyus-Abraham, and E. H. Sargent, ACS Nano **2**, 833 (2008).
[21] M. C. Beard, A. G. Midgett, M. Law, O. E. Semonin, R. J. Ellingson, and A. J. Nozik, Nano Lett. **9**, 836 (2009).
[22] M. Sykora, A. Y. Koposov, J. A. McGuire, R. K. Schulze, O. Tretiak, J. M. Pietryga, and V. I. Klimov, ACS Nano **4**, 2021 (2010).
[23] J. A. McGuire, M. Sykora, J. Joo, J. M. Pietryga, and V. I. Klimov, Nano Lett. **10**, 2049 (2010).
[24] W. A. Tisdale, K. J. Williams, B. A. Timp, D. J. Norris, E. S. Aydil, and X.-Y. Zhu, Science **328**, 1543 (2010).
[25] M. C. Beard, A. G. Midgett, M. C. Hanna, J. M. Luther, B. K. Hughes, and A. J. Nozik, Nano Lett. **9**, 836 (2009).
[26] J.-W. Luo, A. Franceschetti, and A. Zunger, Nano Lett. **8**, 3174 (2008).
[27] C. Delerue, G. Allan, J. J. H. Pijpers, and M. Bonn, Phys. Rev. B **81**, 125306 (2010).
[28] R. Koole, G. Allan, C. Delerue, A. Meijerink, D. Vanmaekelbergh, and A. Houtepen, Small **4**, 127 (2008).
[29] X. Peng, L. Manna, W. Yang, J. Wickham, E. Scher, A. Kadavanich, and A. P. Alivisatos, Nature (London) **404**, 59 (2000).
[30] J. Hu, L.-S. Li, W. Yang, L. Manna, L.-W. Wang, and A. P. Alivisatos, Science **292**, 2060 (2001).
[31] L.-S. Li, J. Hu, W. Yang, and A. P. Alivisatos, Nano Lett. **1**, 349 (2001).
[32] S. Kan, T. Mokari, E. Rothenberg, and U. Banin, Nature Mater. **2**, 155 (2003).
[33] H. Yu, J. Li, R. A. Loomis, L.-W. Wang, and W. E. Buhro, Nature Mater. **2**, 517 (2003).
[34] W.-K. Koh, A. C. Bartnik, F. W. Wise, and C. B. Murray, J. Am. Chem. Soc. **132**, 3909 (2010).
[35] T. Sadowski and R. Ramprasad, Phys. Rev. B **76**, 235310 (2007).
[36] Q. Zhao, P. A. Graf, W. B. Jones, A. Franceschetti, J. Li, L.-W. Wang, and K. Kim, Nano Lett. **7**, 3274 (2007).
[37] Y. Wang, R. Zhang, T. Frauenheim, and T. A. Niehaus, J. Phys. Chem. C **113**, 12935 (2009).
[38] K. F. Karlsson, M. A. Dupertuis, D. Y. Oberli, E. Pelucchi, A. Rudra, P. O. Holtz, and E. Kapon, Phys. Rev. B **81**, 161307 (2010).
[39] N. Zonias, P. Lagoudakis, and C.-K. Skylaris, J. Phys.: Condens. Matter **22**, 025303 (2010).
[40] J. M. Soler, E. Artacho, J. D. Gale, A. García, J. Junquera, P. Ordejón, and D. Sánchez-Portal, J. Phys.: Condens. Matter **14**, 2745 (2002).
[41] N. Troullier and J. L. Martins, Phys. Rev. B **43**, 1993 (1991).
[42] G. Kresse and J. Furthmüller, Phys. Rev. B **54**, 11169 (1996).
[43] S. Meng and E. Kaxiras, J. Chem. Phys. **129**, 054110 (2008).
[44] J. P. Perdew, K. Burke, and M. Ernzerhof, Phys. Rev. Lett. **77**, 3865 (1996).
[45] A. Tsolakidis, D. Sánchez-Portal, and R. M. Martin, Phys. Rev. B **66**, 235416 (2002).
[46] A. Tsolakidis and R. M. Martin, Phys. Rev. B **71**, 125319 (2005).

[47]G. Nesher, L. Kronik, and J. R. Chelikowsky, Phys. Rev. B **71**, 035344 (2005).
[48]B. G. Walker, S. C. Hendy, R. Gebauer, and R. D. Tilley, Eur. Phys. J. B **66**, 7 (2008).
[49]T. J. Pennycook, G. Hadjisavvas, J. C. Idrobo, P. C. Kelires, and S. T. Pantelides, Phys. Rev. B **82**, 125310 (2010).
[50]S.-H. Wei and A. Zunger, Phys. Rev. B **55**, 13605 (1997).
[51]R. Leitsmann and F. Bechstedt, ACS Nano **3**, 3505 (2009).
[52]A. Franceschetti, J. M. An, and A. Zunger, Nano Lett. **6**, 2191 (2006).
[53]G. Allan and C. Delerue, Phys. Rev. B **73**, 205423 (2006).
[54]E. Rabani and R. Baer, Nano Lett. **8**, 4488 (2008).
[55]C. Sevik and C. Bulutay, Phys. Rev. B **77**, 125414 (2008).
[56]G. Allan and C. Delerue, Phys. Rev. B **77**, 125340 (2008).
[57]M. Vörös, A. Gali, D. Rocca, G. Zimanyi, and G. Galli (unpublished).
[58]B. Goller, S. Polisski, H. Wiggers, and D. Kovalev, Appl. Phys. Lett. **97**, 041110 (2010).
[59]A. Gali, M. Vörös, D. Rocca, G. T. Zimanyi, and G. Galli, Nano Lett. **9**, 3780 (2009).
[60]F. Trani, G. Cantele, D. Ninno, and G. Iadonisi, Phys. Rev. B **72**, 075423 (2005).
[61]A. Franceschetti, Phys. Rev. B **78**, 075418 (2008).